

Bayesian Modeling of Collatz Stopping Times: A Probabilistic Machine Learning Perspective

Nicolò Bonacorsi* Matteo Bordoni†

March 6, 2026

Abstract

We study the Collatz total stopping time $\tau(n)$ over $n \leq 10^7$ from a probabilistic machine learning viewpoint. Empirically, $\tau(n)$ is a skewed and heavily overdispersed count with pronounced arithmetic heterogeneity. We develop two complementary models. First, a Bayesian hierarchical Negative Binomial regression (NB2-GLM) predicts $\tau(n)$ from simple covariates ($\log n$ and residue class $n \bmod 8$), quantifying uncertainty via posterior and posterior predictive distributions. Second, we propose a mechanistic generative approximation based on the odd-block decomposition: for odd m , write $3m + 1 = 2^{K(m)}m'$ with m' odd and $K(m) = v_2(3m + 1) \geq 1$; randomizing these block lengths yields a stochastic approximation calibrated via a Dirichlet-multinomial update. On held-out data, the NB2-GLM achieves substantially higher predictive likelihood than the odd-block generators. Conditioning the block-length distribution on $m \bmod 8$ markedly improves the generator's distributional fit, indicating that low-order modular structure is a key driver of heterogeneity in $\tau(n)$.

1 Introduction

Let $T : \mathbb{N} \rightarrow \mathbb{N}$ be the Collatz map

$$T(n) = \begin{cases} n/2, & n \text{ even,} \\ 3n + 1, & n \text{ odd,} \end{cases}$$

and define the total stopping time

$$\tau(n) = \min\{t \geq 0 : T^t(n) = 1\}.$$

The Collatz conjecture asserts $\tau(n) < \infty$ for all n and remains open [1–4]. Here we do not attempt to prove the conjecture. Instead we treat n as random and study the induced empirical law of $\tau(n)$ over a large range.

*Department of Applied Mathematics, Columbia University, New York, USA. Email: nb3328@columbia.edu

†Department of Mathematics, Columbia University, New York, USA. Email: mb5333@columbia.edu

Dataset and question. We fix $N = 10^7$ and compute $\tau(n)$ for all $1 \leq n \leq N$, yielding $\mathcal{D}_N = \{(n, \tau(n))\}_{n=1}^N$. Our goal is predictive and explanatory: *which simple probabilistic models can predict and explain the observed distributional shape of $\tau(n)$ and its arithmetic heterogeneity?*

Two complementary models. We develop: (i) a Bayesian hierarchical Negative Binomial regression treating $\tau(n)$ as an overdispersed count whose conditional mean depends on $\log n$ and $n \bmod 8$ (Section 3); and (ii) a mechanistic generative odd-block model that randomizes the block-lengths $K = v_2(3m + 1)$ in the accelerated odd-to-odd dynamics (Section 4). Section 5 compares predictive performance on held-out data. Further rationale for the regressors and the odd-block heuristics is given in Appendix C.

A note on randomness (working likelihood). The map T and the stopping time $\tau(n)$ are deterministic. Throughout, the term “probabilistic model” is used in the standard statistical sense of a *working likelihood*: we treat n as random (e.g. uniformly sampled from $\{1, \dots, N\}$ in our evaluation), and we model the induced variability of $\tau(n)$ across n by a parametric stochastic family. This provides uncertainty quantification and principled predictive comparisons, without positing physical noise in the Collatz dynamics.

2 Data and exploratory analysis

Computing $\tau(n)$ at scale

A direct simulation for every $n \leq 10^7$ is expensive due to long trajectories. We use dynamic programming: while computing $\tau(i)$, if the orbit hits some $m < i$, we stop and set $\tau(i) = k + \tau(m)$, reusing cached values. Numba JIT compilation accelerates the core loop [5]. Details are in Appendix A.

Distributional shape and overdispersion

Figure 1 summarizes the marginal distribution of $\tau(n)$ (histogram with integer-aligned bins plus KDE overlay). The heavy right tail motivates an overdispersed count likelihood. Table 1 reports key summaries for $N = 10^7$, including the dispersion ratio $R = \widehat{\text{Var}}(\tau)/\widehat{\mathbb{E}}[\tau] \approx 24.56 \gg 1$, ruling out Poisson as a realistic noise model [6, 7].

Scale effect and arithmetic heterogeneity

Figure 2 plots $\tau(n)$ versus n on a log- x axis: the mean grows slowly with n and the spread increases (heteroskedasticity). The visible banding reflects arithmetic structure; one robust proxy is the residue class modulo a small power of two, motivating $n \bmod 8$ as a low-dimensional categorical feature in the regression model.

3 Method 1: Bayesian Negative Binomial regression

The empirical $R \gg 1$ suggests a Negative Binomial likelihood. We use the NB2 mean-dispersion parameterization: conditional on (μ_n, α) ,

$$Y_n = \tau(n) \mid \mu_n, \alpha \sim \text{NB}(\mu_n, \alpha), \quad \mathbb{E}[Y_n \mid \mu_n, \alpha] = \mu_n, \quad \text{Var}(Y_n \mid \mu_n, \alpha) = \mu_n + \alpha \mu_n^2,$$

with parameter mappings and a PyMC implementation note in Appendix D.

Hierarchical NB2-GLM

We link μ_n to covariates via a log-link and include a random intercept by residue class modulo 8:

$$\log \mu_n = \eta_n, \tag{1}$$

$$\eta_n = \beta_0 + \beta_{\log} \log n + u_{\text{mod}8(n)}, \tag{2}$$

$$u_r \mid \sigma_u \sim \mathcal{N}(0, \sigma_u^2), \quad r = 0, 1, \dots, 7. \tag{3}$$

This hierarchical structure performs partial pooling across congruence classes, producing stable class-specific deviations while controlling overfitting.

Inference and predictive evaluation

We use weakly-informative priors and fully specify them in Appendix B.2. We fit with NUTS [8] in PyMC [9] on a training subsample of size $N_{\text{fit}} = 50,000$ and evaluate on a disjoint test subsample of size $N_{\text{test}} = 50,000$. Both subsamples are drawn uniformly without replacement from $\{1, \dots, N\}$ using a fixed RNG seed (see Appendix B for the exact protocol). For MCMC we run 2 chains with 1000 tuning steps and 1000 draws per chain, and target acceptance 0.9.

Figure 3 shows a held-out posterior predictive check (PPC): the model matches the bulk distribution well and slightly inflates the far right tail, consistent with the quadratic NB2 variance.

4 Method 2: A stochastic odd-block generative model

Regression is predictive but phenomenological. We therefore build a mechanistic approximation based on the odd-block decomposition. When m is odd, $3m + 1$ is even and can be written

$$3m + 1 = 2^{K(m)} m', \quad m' \text{ odd}, \quad K(m) = v_2(3m + 1) \geq 1.$$

Thus one odd update is followed by $K(m)$ halving steps until returning to an odd state.

Accelerated odd-to-odd dynamics

Let m_0 be the first odd iterate encountered from n (after $v_2(n)$ initial halvings). Define the accelerated map

$$m_{j+1} = \frac{3m_j + 1}{2^{K(m_j)}}.$$

The total stopping time decomposes as

$$\tau(n) = v_2(n) + \sum_{j=0}^{J-1} (1 + K(m_j)),$$

where J is the first index such that $m_J = 1$. This identity is exact for the deterministic dynamics.

Randomized block-length generator

The generative approximation replaces $K(m_j)$ by a stochastic sequence (K_j) with pmf $(p_k)_{k \geq 1}$:

$$M_{j+1} \approx \left\lfloor \frac{3M_j + 1}{2^{K_j}} \right\rfloor_{\text{odd}}, \quad \tau_{\text{gen}}(n) = v_2(n) + \sum_{j=0}^{J-1} (1 + K_j). \quad (4)$$

The rounding $\lfloor \cdot \rfloor_{\text{odd}}$ mirrors the implementation detail that the stochastic update can produce an even intermediate due to integer arithmetic, and we project back to the odd state space to preserve the odd-to-odd structure.

A classical heuristic suggests K is close to geometric with $\mathbb{P}(K = k) \approx 2^{-k}$, $k \geq 1$. Under this reference, $\mathbb{E}[3/2^K] = 1$ but the log-drift is negative (Appendix F), consistent with contraction on a log scale.

Definition of the odd projection $\lfloor \cdot \rfloor_{\text{odd}}$. In the generator we implement the odd-to-odd update by first rounding to the nearest integer and then projecting to the odd state space: let $\lfloor x \rfloor$ denote rounding to the nearest integer (ties to even), and define

$$\lfloor x \rfloor_{\text{odd}} = \begin{cases} 1, & \lfloor x \rfloor \leq 1, \\ \lfloor x \rfloor, & \lfloor x \rfloor \text{ odd}, \\ \lfloor x \rfloor + 1, & \lfloor x \rfloor \text{ even and } \lfloor x \rfloor > 1. \end{cases}$$

This matches the implementation used to generate the results in Section 5.

Calibrating p_k and posterior predictive checks

We estimate p_k from observed block lengths $K_i = v_2(3m_i + 1)$ using a Dirichlet prior, yielding a conjugate Dirichlet posterior [10] (Appendix E).

In implementation we discretize K on $\{1, \dots, K_{\text{max}}\}$ with $K_{\text{max}} = 30$ by capping $K_{\text{cap}} = \min(K, K_{\text{max}})$, so the last category aggregates the tail event $\{K \geq K_{\text{max}}\}$. We use a symmetric Dirichlet prior with concentration $\alpha_k = 1$ for $k = 1, \dots, K_{\text{max}}$.

Figure 4 compares empirical frequencies to the geometric reference on a log scale; this directly tests the key modeling assumption. Figure 5 shows posterior uncertainty on (p_k) . Figure 7 compares the generated stopping-time distributions to empirical stopping times via a distributional PPC.

5 Model comparison: predictive accuracy vs. mechanistic faithfulness

Posterior predictive checks are qualitative. To compare the regression and generative approaches on equal footing we use a *proper scoring rule* [11] on held-out data: the log predictive score. On a test set $\{(n_i, y_i)\}_{i=1}^{N_{\text{test}}}$ with $y_i = \tau(n_i)$, define

$$\text{Score} = \sum_{i=1}^{N_{\text{test}}} \log p(y_i | n_i, \mathcal{D}_{\text{fit}}).$$

For the NB2-GLM, $p(y_i | n_i, \mathcal{D}_{\text{fit}})$ is obtained by averaging the NB pmf over posterior draws. For the odd-block generator, we estimate a predictive pmf by Monte Carlo simulation: $\hat{p}_i(y) = \frac{1}{S_{\text{MC}}} \sum_{s=1}^{S_{\text{MC}}} \mathbf{1}\{\tau_{\text{gen}}^{(s)}(n_i) = y\}$ and score $\sum_i \log(\hat{p}_i(y_i) + \varepsilon)$ with $\varepsilon = 10^{-12}$ for numerical stability. We use $S_{\text{MC}} = 40$ Monte Carlo replicates per test point. We emphasize that the generator log score is a Monte Carlo approximation to the ideal log predictive score, since $\hat{p}_i(y_i)$ is estimated from finitely many replicates.

In addition, we report a distributional distance between empirical and predictive CDFs (1-Wasserstein [12]) to summarize global shape mismatch. Table 2 provides the reporting format.

Interpretation. Table 2 shows that the hierarchical NB2-GLM achieves by far the best predictive likelihood on the held-out set: its log score is -2.73×10^5 (average -5.46 per observation), compared to -1.17×10^6 for the global odd-block generator G2 and -1.08×10^6 for the conditional generator G3. In other words, the regression model assigns substantially higher probability to the realized stopping times. In terms of distributional fit, the NB2-GLM also attains the smallest W_1 distance ($W_1 \approx 3.20$), with G3 improving markedly over G2 ($W_1 \approx 5.43$ vs. 17.59) but still lagging behind the regression.

From a purely predictive, proper-score perspective, the NB2-GLM (M3) is therefore the best model among those considered. However, the odd-block generator remains attractive from a mechanistic point of view: it explains heavy tails and heterogeneity through randomized block lengths $K = v_2(3m + 1)$ and their arithmetic dependence on $m \bmod 8$. The conditional variant G3 narrows the gap in predictive performance while preserving this structural interpretation, making it a natural candidate when mechanistic faithfulness is prioritized over raw log score.

6 Discussion

Two complementary conclusions emerge. First, a compact hierarchical NB2-GLM with $\log n$ and $n \bmod 8$ captures much of the predictive structure of $\tau(n)$, with uncertainty quantification via the posterior and PPC (Figure 3). Second, the odd-block decomposition yields a mechanistic generator whose success hinges on accurately modeling the distribution of $K = v_2(3m + 1)$ and its arithmetic dependence (Figures 4–7). The conditional variant provides a bridge between the two viewpoints: modular structure that appears as a random effect in regression becomes explicit conditioning information in the generator.

Future work includes extending the conditional structure to higher powers of two, incorporating explicit state-dependence in (K_j) , and using likelihood-based calibration of the generator to align scoring-rule performance with mechanistic interpretability.

References

- [1] Jeffrey C Lagarias. The $3x + 1$ problem and its generalizations. *The American Mathematical Monthly*, 92(1):3–23, 1985.
- [2] Terence Tao. Almost all orbits of the collatz map attain almost bounded values. *Forum of Mathematics, Pi*, 10:e12, 2022. doi: 10.1017/fmp.2022.8.
- [3] Riho Terras. A stopping time problem on the positive integers. *Acta Arithmetica*, 30(3): 241–252, 1976.
- [4] Ya. G. Sinai. Statistical $(3x + 1)$ problem. *Communications on Pure and Applied Mathematics*, 56(7):1016–1028, 2003. doi: 10.1002/cpa.10084.
- [5] Siu Kwan Lam, Antoine Pitrou, and Stanley Seibert. Numba: A llvm-based python jit compiler. In *Proceedings of the Second Workshop on the LLVM Compiler Infrastructure in HPC*, pages 1–6, 2015.
- [6] A Colin Cameron and Pravin K Trivedi. *Regression analysis of count data*. Cambridge University Press, 2nd edition, 2013.
- [7] Andrew Gelman, John B Carlin, Hal S Stern, David B Dunson, Aki Vehtari, and Donald B Rubin. *Bayesian data analysis*. CRC press, 3rd edition, 2013.
- [8] Matthew D Hoffman and Andrew Gelman. The no-u-turn sampler: adaptively setting path lengths in hamiltonian monte carlo. *Journal of Machine Learning Research*, 15(1): 1593–1623, 2014.
- [9] Oriol Abril-Pla et al. PyMC: A modern, and comprehensive probabilistic programming framework in python. *PeerJ Computer Science*, 9:e1516, 2023.
- [10] Kevin P Murphy. *Machine learning: a probabilistic perspective*. MIT press, 2012.
- [11] Tilmann Gneiting and Adrian E Raftery. Strictly proper scoring rules, prediction, and estimation. *Journal of the American statistical Association*, 102(477):359–378, 2007.
- [12] Cédric Villani. *Optimal transport: old and new*. Springer Science & Business Media, 2009.

Appendix

A Method to construct the dataset

A naive implementation of the stopping-time computation is too slow when N is as large as 10^7 , due to the potentially long trajectories required for some starting values. To obtain a scalable engine, we use Python together with NumPy arrays and Numba’s just-in-time (JIT) compilation [5]. Numba compiles the core loops to efficient machine code, drastically reducing Python overhead and enabling the computation of $\tau(n)$ for all $n \leq N$ within a standard Colab-like runtime.

We also exploit a dynamic-programming shortcut. When computing $\tau(i)$ for a given i , the trajectory (n_k) may eventually visit a value $m < i$. At that point the remaining number of steps to reach 1 is exactly $\tau(m)$, which has already been computed earlier. Thus we can terminate the iteration and set

$$\tau(i) = k + \tau(m),$$

reusing cached values. This reuse is particularly effective for large N , where many trajectories merge into segments already explored.

The output of this stage is the dataset

$$\mathcal{D}_N = \{(n, \tau(n)) : 1 \leq n \leq N\},$$

stored as a table with N rows. In later analysis we augment each row with simple derived features of n (e.g. $\log n$ and $n \bmod 8$) to serve as covariates in the regression model.

B Reproducibility details (splits, priors, and evaluation)

B.1 Train/test protocol

We draw $N_{\text{fit}} = 50,000$ indices uniformly without replacement from $\{1, \dots, N\}$ using RNG seed 123, and set the remaining pool as candidates for testing. We then draw $N_{\text{test}} = 50,000$ test indices uniformly without replacement from the remaining pool, again using the same RNG stream.

B.2 Priors and MCMC settings for M3

For the hierarchical NB2-GLM (M3) we use:

$$\beta_0 \sim \mathcal{N}(0, 10^2), \quad \beta_{\log} \sim \mathcal{N}(0, 5^2), \quad \sigma_u \sim \text{HalfNormal}(1), \quad \alpha \sim \text{HalfNormal}(5),$$

with $u_r = \sigma_u z_r$, $z_r \sim \mathcal{N}(0, 1)$ for $r = 0, \dots, 7$. We sample with NUTS (PyMC) using 2 chains, 1000 tuning steps and 1000 posterior draws per chain, target acceptance 0.9, and a fixed random seed.

B.3 Generator evaluation settings

For the odd-block generators we cap the simulated stopping-time loop at `MAX_STEPS = 200,000` steps to avoid pathological non-absorption under the stochastic approximation. Log scores use $S_{MC} = 40$ Monte Carlo replicates per test point, $\varepsilon = 10^{-12}$, and fixed RNG seeds for exact reproducibility.

C Modeling choices and heuristics (rationale)

This appendix explains the main modeling choices in the paper: (i) the regressors used in the NB2-GLM, (ii) the Negative Binomial likelihood, and (iii) the design of the odd-block generator and its variants. The goal is not to add new theory, but to make the modeling decisions transparent and defensible.

C.1 Why model $\tau(n)$ as an overdispersed count (NB2 rather than Poisson)

The response $\tau(n)$ is a nonnegative integer-valued quantity, so a count likelihood is natural. A Poisson model would impose $\text{Var}(Y | x) \approx \mathbb{E}[Y | x]$, which is strongly violated in our data: the empirical dispersion ratio $\widehat{\text{Var}}(\tau)/\widehat{\mathbb{E}}[\tau]$ is far above 1 (Table 1). This motivates a Negative Binomial likelihood, which allows variance to grow faster than the mean.

We use the NB2 mean–dispersion parameterization

$$\text{Var}(Y | \mu, \alpha) = \mu + \alpha\mu^2,$$

because it captures two empirically visible features simultaneously: (i) strong overdispersion and (ii) increasing spread at larger conditional means (heteroskedasticity). In practice, NB2 is also a standard default in applied count regression when the data show heavy tails and variance inflation.

C.2 Why $\log n$ as the main scale regressor

A basic empirical fact is that $\tau(n)$ grows slowly with n but not linearly (Figure 2). Using n directly as a regressor would force the model to allocate too much curvature to match a trend that is visually closer to logarithmic. The transformation $\log n$ provides a simple one-dimensional scale summary that: (i) compresses the dynamic range $1 \leq n \leq 10^7$, (ii) matches the observed slow growth of typical stopping times, and (iii) yields stable numerical inference under a log-link.

In short, $\log n$ is the minimal scale feature that captures the macro-trend without introducing a flexible nonlinear basis that would be harder to interpret or justify, allowing us to maintain model parsimony and interpretability.

C.3 Why include residue class $n \bmod 8$ (and why as a random effect)

Beyond scale effects, Collatz dynamics exhibit visible arithmetic stratification: values of $\tau(n)$ form bands when plotted against n (Figure 2), indicating that a coarse modular signature already explains a nontrivial part of the heterogeneity. We use $n \bmod 8$ as a low-dimensional categorical covariate because:

- It is a minimal “power-of-two” modular feature (small enough to avoid a high-dimensional categorical design),
- It aligns with the prominence of 2-adic structure in Collatz steps (repeated halving), and
- It is empirically robust: the banding is clearly visible already at this resolution.

We model the eight class offsets as a hierarchical (partially pooled) random effect $u_r \sim \mathcal{N}(0, \sigma_u^2)$ rather than eight unrelated fixed effects. This choice stabilizes inference and prevents overfitting by shrinking class-specific deviations toward 0 when the data provide weak evidence for large differences. It also matches the modeling goal: we want to quantify that “mod 8 matters” while keeping the model small.

C.4 Why we did not add more regressors

Additional predictors are possible (e.g. $v_2(n)$, richer residue classes, or nonlinear functions of $\log n$). We deliberately keep the regression model compact to preserve interpretability: the point is not to maximize predictive accuracy at any cost, but to demonstrate that a minimal set of theoretically motivated covariates already yields strong predictive performance and useful uncertainty quantification.

C.5 Odd-block generator: why it is a natural mechanistic approximation

The odd-block decomposition isolates the only “expanding” step (odd $\mapsto 3m + 1$) from the subsequent sequence of deterministic halving steps. For odd m , writing $3m + 1 = 2^{K(m)}m'$ with m' odd turns the dynamics into odd-to-odd jumps plus a block length $K(m)$. This motivates a mechanistic approximation where the complicated deterministic dependence of $K(m)$ on m is replaced by a stochastic surrogate distribution.

The baseline heuristic $\Pr(K = k) \approx 2^{-k}$ corresponds to the intuition that $3m + 1$ behaves roughly like a “random even integer” in its 2-adic valuation, so the number of factors of 2 is approximately geometric. The calibrated variants (G2/G3) keep the same mechanism but estimate the block-length distribution from data, making the approximation testable rather than purely heuristic.

C.6 Why conditioning on $m \bmod 8$ is the first meaningful refinement

The global i.i.d. block-length model (G2) averages over strong arithmetic heterogeneity. A minimal refinement is to condition p_k on a low-order residue class that is directly tied to 2-adic structure. Conditioning on $m \bmod 8$ is the smallest such choice that is still informative: it is low-dimensional (8 classes) but already captures systematic differences in the estimated block-length distribution (Figure 6). The improved PPC and reduced W_1 distance for G3 indicate that the generator benefits substantially from this modular information.

C.7 Why these evaluation metrics

We report two complementary diagnostics:

- **Log predictive score** (proper scoring rule): it evaluates the entire predictive distribution, rewarding models that assign higher probability to the observed outcomes. This is the main principled metric for predictive comparison.
- W_1 (**1-Wasserstein**) **distance**: it summarizes global distributional mismatch between the empirical and predictive marginals, which is particularly informative when heavy tails are present and visual PPCs show shape differences.

For the odd-block generator, the predictive distribution is not available in closed form, so the log score is estimated by Monte Carlo “hit” frequencies at each test point, with S_{MC} replicates. This yields an approximation to a proper score; increasing S_{MC} tightens the estimate at higher computational cost.

D Negative Binomial regression: parameterizations and properties

This appendix summarizes the Negative Binomial (NB) distribution and the NB generalized linear model (GLM) conventions used in the main text.

D.1 Classical (r, p) parameterization

The classical Negative Binomial distribution can be defined as the distribution of the number of failures Y observed before the r -th success in i.i.d. Bernoulli trials with success probability $p \in (0, 1)$:

$$Y \sim \text{NB}(r, p), \quad r > 0, p \in (0, 1).$$

Its pmf is

$$\Pr(Y = y \mid r, p) = \frac{\Gamma(y + r)}{\Gamma(r) \Gamma(y + 1)} (1 - p)^y p^r, \quad y = 0, 1, 2, \dots,$$

and

$$\mathbb{E}[Y] = r \frac{1 - p}{p}, \quad \text{Var}(Y) = r \frac{1 - p}{p^2}.$$

D.2 Mean–dispersion (μ, α) parameterization (NB2)

For regression we use the NB2 convention

$$\mathbb{E}[Y \mid \mu, \alpha] = \mu, \quad \text{Var}(Y \mid \mu, \alpha) = \mu + \alpha \mu^2,$$

where $\alpha > 0$ controls overdispersion and $\alpha \rightarrow 0$ yields the Poisson limit. The mapping to (r, p) is

$$r = \frac{1}{\alpha}, \quad p = \frac{1}{1 + \alpha\mu}.$$

D.3 Implementation note: mapping to PyMC

In PyMC, `NegativeBinomial(mu=mu, alpha=alpha_PyMC)` uses

$$\text{Var}(Y \mid \mu, \alpha_{\text{PyMC}}) = \mu + \frac{\mu^2}{\alpha_{\text{PyMC}}}.$$

Therefore, to match the NB2 convention above we set

$$\alpha_{\text{PyMC}} = \frac{1}{\alpha}.$$

D.4 Poisson–Gamma mixture view

If $\Lambda \sim \text{Gamma}(r, c)$ and $Y \mid \Lambda \sim \text{Poisson}(\Lambda)$, then $Y \sim \text{NB}(r, p)$ with $p = c/(c + 1)$. In NB2 form, taking $r = \alpha^{-1}$ and $c = \alpha^{-1}/\mu$ recovers $\text{Var}(Y) = \mu + \alpha\mu^2$, interpreting overdispersion as latent rate heterogeneity.

E Dirichlet–multinomial update

If K_1, \dots, K_m are i.i.d. categorical with probabilities $p_1, \dots, p_{K_{\max}}$ and prior $p \sim \text{Dir}(\alpha)$, the posterior is $\text{Dir}(\alpha + c)$ with $c_k = \sum_{i=1}^m \mathbf{1}\{K_i = k\}$. Posterior means and variances are

$$\mathbb{E}[p_k \mid K_{1:m}] = \frac{\alpha_k + c_k}{\sum_j (\alpha_j + c_j)}, \quad \text{Var}(p_k \mid K_{1:m}) = \frac{(\alpha_k + c_k)(\alpha_0 + m - (\alpha_k + c_k))}{(\alpha_0 + m)^2(\alpha_0 + m + 1)},$$

where $\alpha_0 = \sum_j \alpha_j$.

F Log-scale random walk approximation

Ignoring the additive +1 term for large states, the odd-block update satisfies $M_{j+1} \approx (3/2^{K_j})M_j$, hence in logarithmic scale

$$X_{j+1} \approx X_j + \log_2 3 - K_j, \quad X_j = \log_2 M_j.$$

Even when $\mathbb{E}[3/2^K] = 1$, Jensen’s inequality implies $\mathbb{E}[\log_2(3/2^K)] < \log_2 \mathbb{E}[3/2^K] = 0$, yielding a negative drift in X_j and suggesting absorption at small values is typical.

List of Figures

1	Empirical distribution of $\tau(n)$ for $1 \leq n \leq N$ (integer-aligned bins, width 2) with a KDE overlay computed on a large subsample to reduce noise. This motivates an overdispersed count likelihood.	13
2	Scatter of $\tau(n)$ vs. n (log- x). The mean increases slowly and is approximately linear as a function of $\log n$, while the spread grows with n ; banding suggests modular structure, motivating $\log n$ and $n \bmod 8$ as covariates.	13
3	Posterior predictive check for the hierarchical NB2-GLM (Model M3). The PPC matches the bulk well and mildly overestimates extreme right-tail mass.	14
4	Empirical block-length distribution \hat{p}_k for $K = v_2(3m + 1)$ (odd $m \leq N$) vs. geometric reference 2^{-k} on log- y . This evaluates the “geometric K ” heuristic.	14
5	Dirichlet posterior for (p_k) (log scale) with uncertainty bars, compared to the geometric reference 2^{-k}	15
6	Posterior mean of p_k conditional on the odd residue class $m \bmod 8$ (heatmap). This reveals systematic arithmetic dependence beyond an i.i.d. geometric law.	15
7	PPC overlay: empirical τ vs. G1 (geometric 2^{-k}), G2 (global calibrated p_k), and G3 (p_k conditional on $m \bmod 8$). Conditioning reduces the bias in the mean and improves distributional agreement in the bulk.	16
8	Example trajectory in log scale for $n = 27$: deterministic Collatz vs. stochastic odd-block approximation.	16

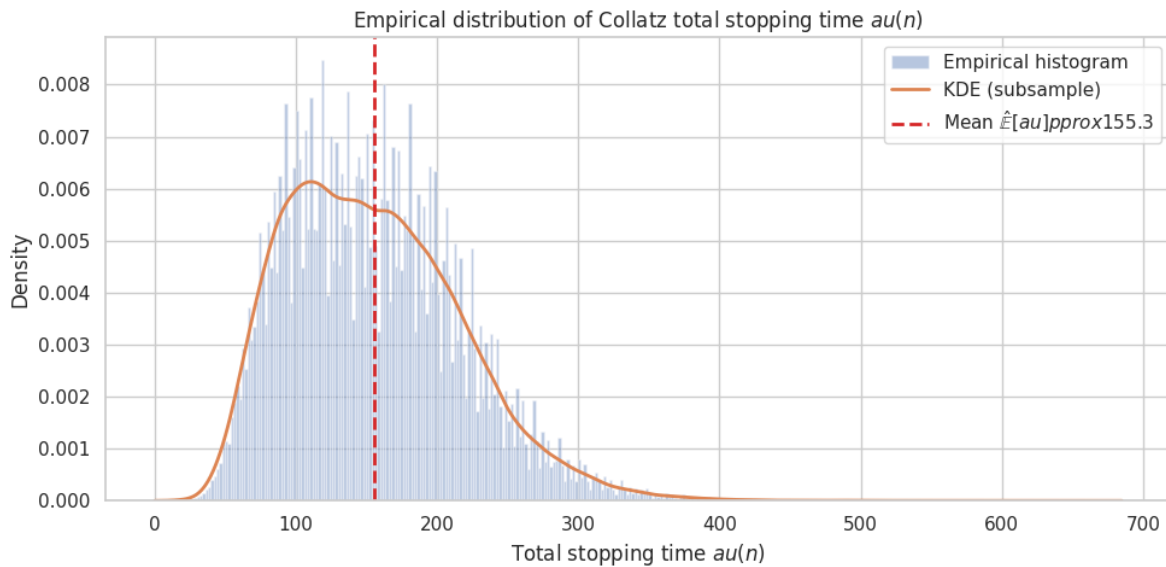


Figure 1: Empirical distribution of $\tau(n)$ for $1 \leq n \leq N$ (integer-aligned bins, width 2) with a KDE overlay computed on a large subsample to reduce noise. This motivates an overdispersed count likelihood.

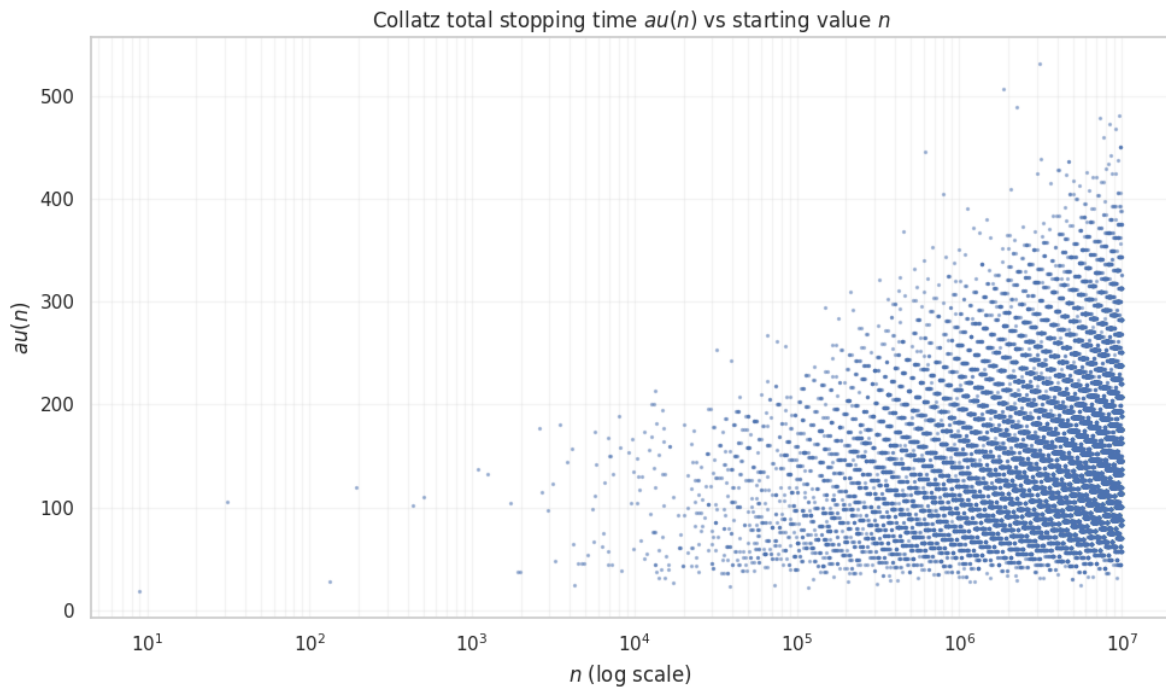


Figure 2: Scatter of $\tau(n)$ vs. n ($\log-x$). The mean increases slowly and is approximately linear as a function of $\log n$, while the spread grows with n ; banding suggests modular structure, motivating $\log n$ and $n \bmod 8$ as covariates.

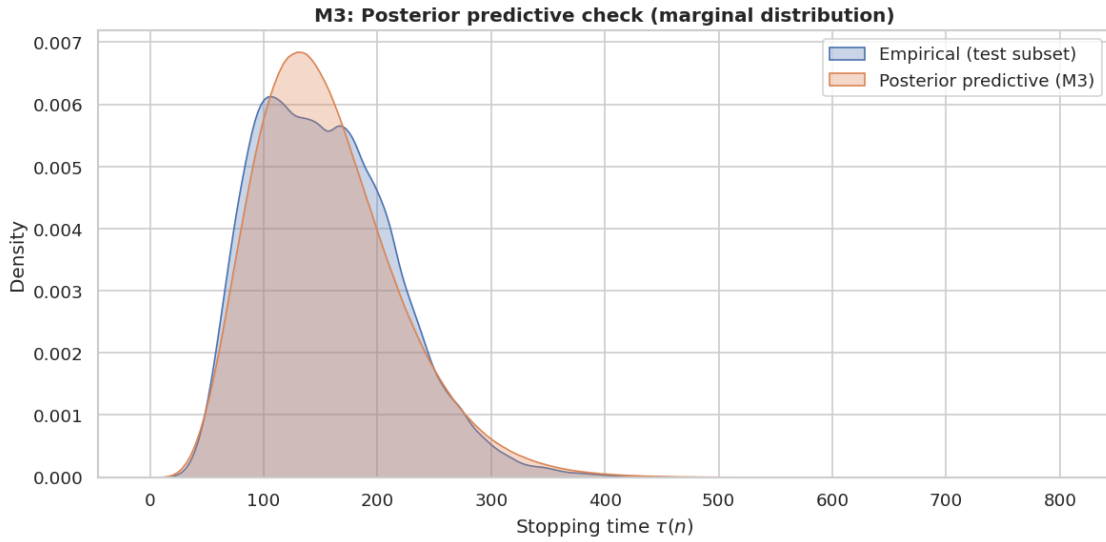


Figure 3: Posterior predictive check for the hierarchical NB2-GLM (Model M3). The PPC matches the bulk well and mildly overestimates extreme right-tail mass.

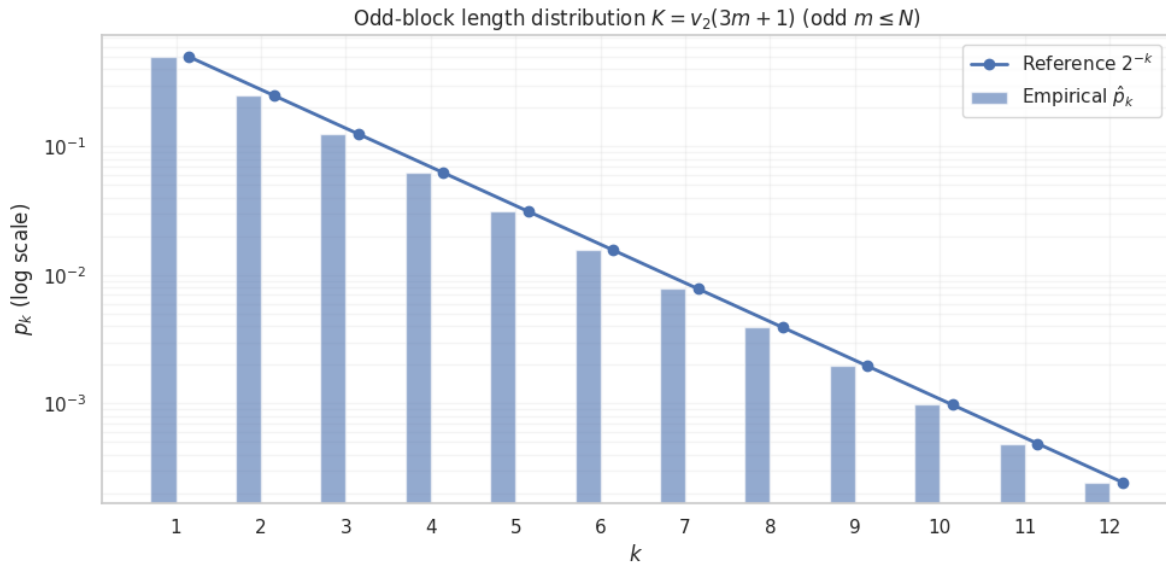


Figure 4: Empirical block-length distribution \hat{p}_k for $K = v_2(3m + 1)$ (odd $m \leq N$) vs. geometric reference 2^{-k} on log- y . This evaluates the “geometric K ” heuristic.

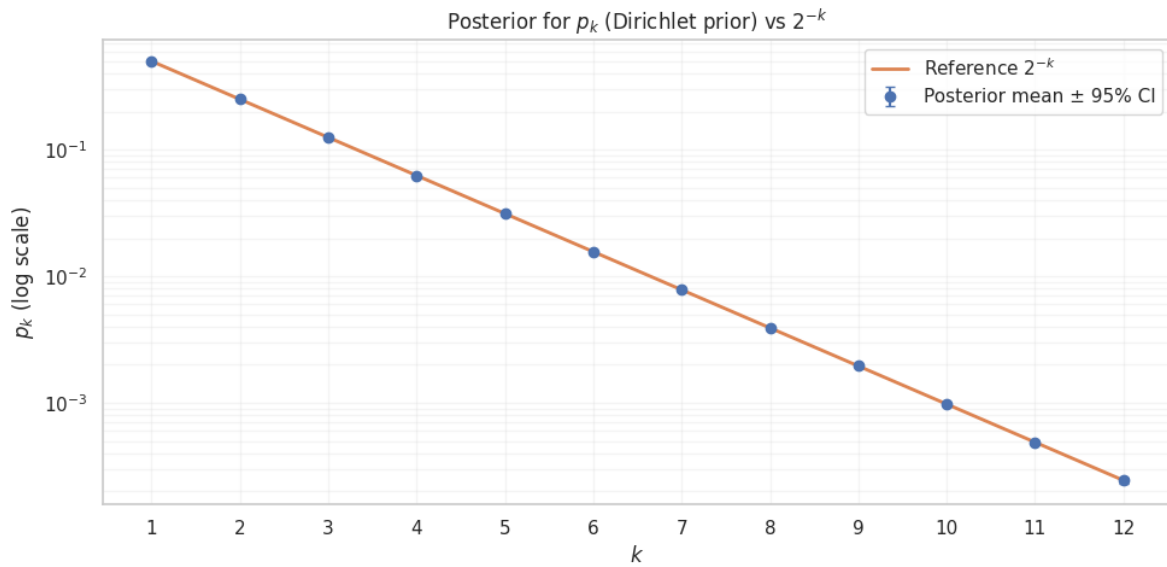


Figure 5: Dirichlet posterior for (p_k) (log scale) with uncertainty bars, compared to the geometric reference 2^{-k} .

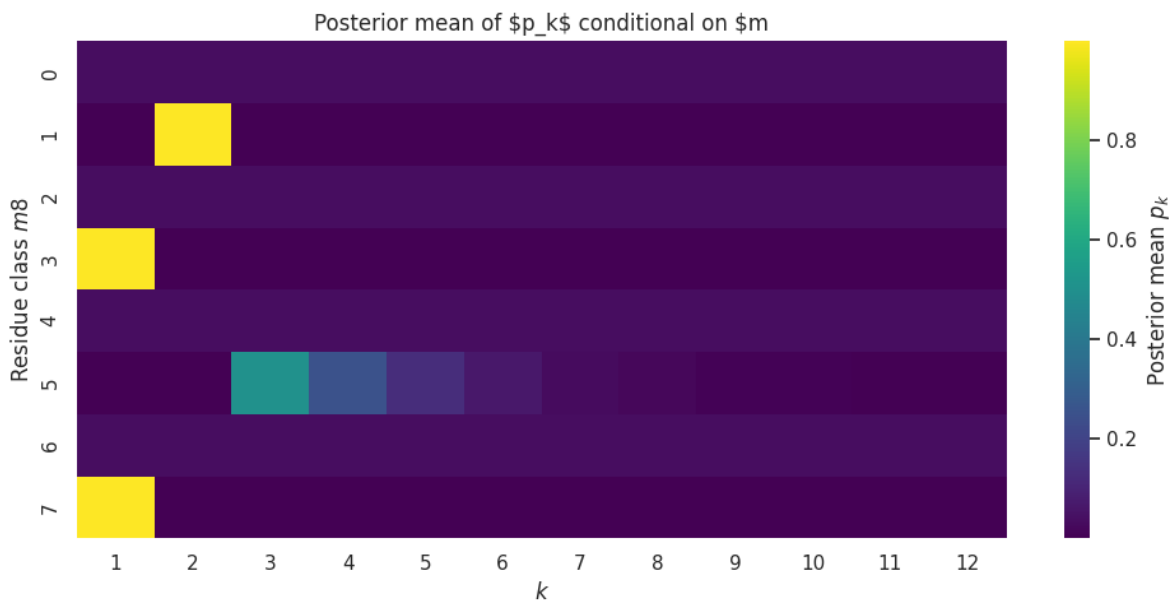


Figure 6: Posterior mean of p_k conditional on the odd residue class $m \pmod{8}$ (heatmap). This reveals systematic arithmetic dependence beyond an i.i.d. geometric law.

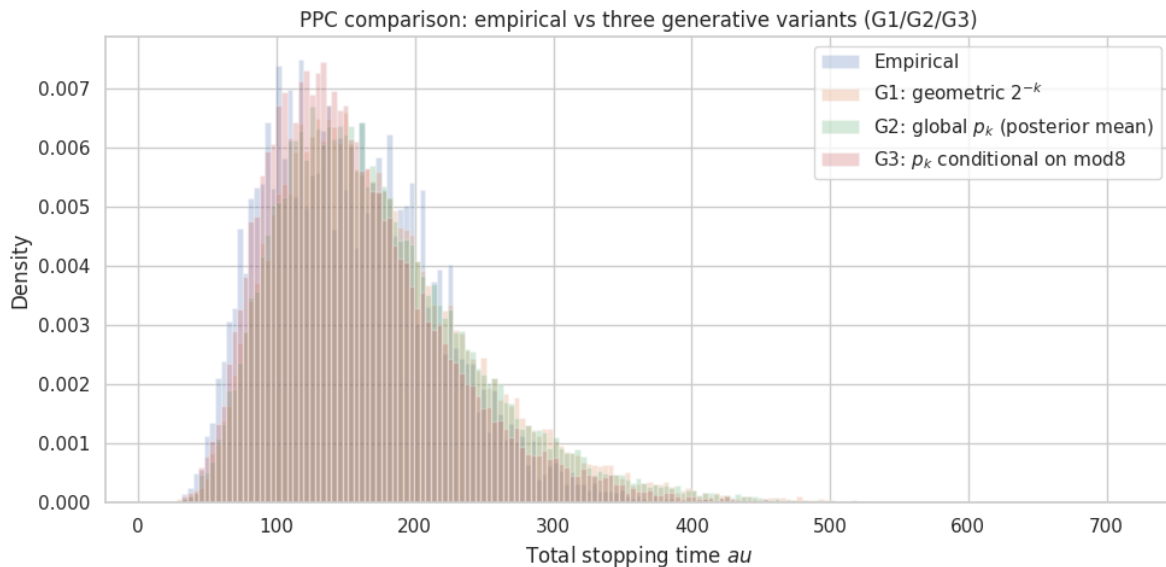


Figure 7: PPC overlay: empirical τ vs. G1 (geometric 2^{-k}), G2 (global calibrated p_k), and G3 (p_k conditional on $m \bmod 8$). Conditioning reduces the bias in the mean and improves distributional agreement in the bulk.

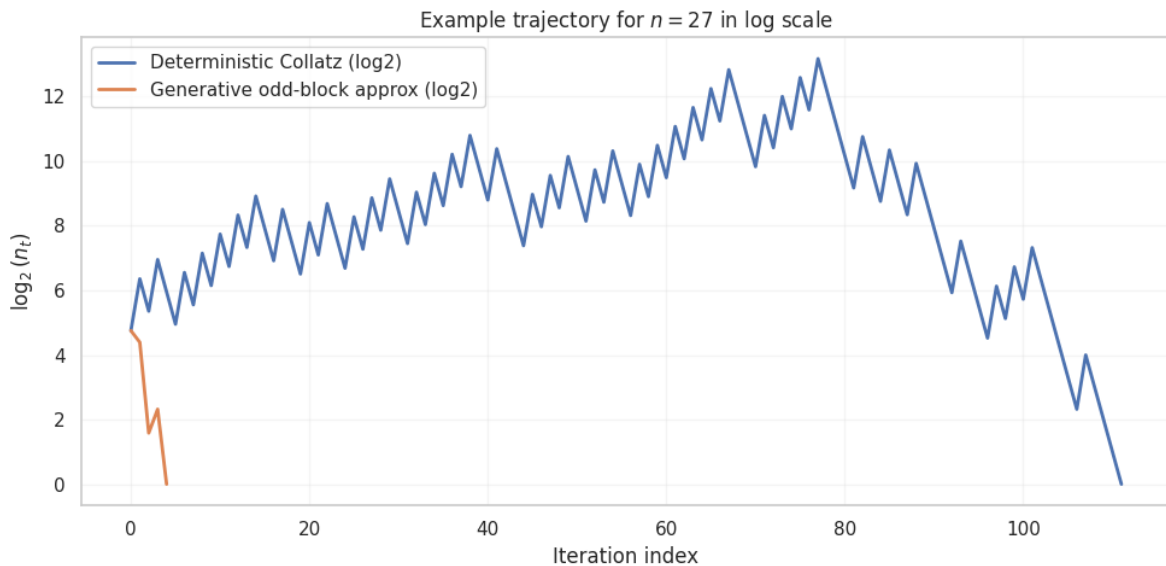


Figure 8: Example trajectory in log scale for $n = 27$: deterministic Collatz vs. stochastic odd-block approximation.

List of Tables

1	Summary statistics for $\tau(n)$ over $1 \leq n \leq N$	18
2	Quantitative comparison on held-out data using a proper log predictive score and a distributional distance. All scores are computed on $N_{\text{test}} = 50,000$ held-out pairs, with the generative log scores estimated via $S_{\text{MC}} = 40$ Monte Carlo replicates per test point.	18

Statistic	Value
N	10,000,000
τ_{\min}	0
τ_{\max}	685
$\widehat{\mathbb{E}}[\tau]$	155.272
$\widehat{\text{Var}}(\tau)$	3814.045
$\widehat{\text{Var}}(\tau)/\widehat{\mathbb{E}}[\tau]$	24.564

Table 1: Summary statistics for $\tau(n)$ over $1 \leq n \leq N$.

Model	Log score (higher better)	W_1 distance (lower better)
NB2-GLM (M3)	-272 911.95	3.199
Odd-block G2 (global p_k)	-1 165 983.43	17.594
Odd-block G3 ($p_k \mid m \bmod 8$)	-1 079 086.65	5.434

Table 2: Quantitative comparison on held-out data using a proper log predictive score and a distributional distance. All scores are computed on $N_{\text{test}} = 50,000$ held-out pairs, with the generative log scores estimated via $S_{\text{MC}} = 40$ Monte Carlo replicates per test point.